Desalination 621 (2026) 119670

Contents lists available at ScienceDirect

Desalination

journal homepage: www.elsevier.com/locate/desal

Energy efficiency of single-pass electrodialysis and nanofiltration/reverse osmosis for brackish water desalination: An experimental comparison

Youssef-Amine Boussouga [a,1], Ramatisa Ladeia Ramos [a], Emmanuel O. Ogunniyi [b], Bryce S. Richards [b], Andrea I. Schäfer [a,*]

[a] Institute for Advanced Membrane Technology (IAMT), Karlsruhe Institute of Technology (KIT), Hermann-von-Helmholtz-Platz 1, 76344, Eggenstein-Leopoldshafen, Germany
[b] Institute of Microstructure Technology (IMT), Karlsruhe Institute of Technology (KIT), Hermann-von-Helmholtz-Platz 1, 76344, Eggenstein-Leopoldshafen, Germany

HIGHLIGHTS

- SPED and NF/RO systems were compared for brackish water desalination
- Reducing the recovery of NF/RO from 30 to 10 % improved permeate quality and SEC
- At 50 % recovery, SPED achieved <1 g/L permeate TDS for salinities up to 15 g/L
- RO at 10 % recovery achieved <1 g/L permeate TDS for salinities up to 17.5 g/L
- SPED was overall more energy efficient compared to NF/RO

GRAPHICAL ABSTRACT

ARTICLE INFO

Keywords:
Pressure-driven membrane
Ion-exchange membrane
Thermodynamic limit
Specific energy consumption
Small-scale system

ABSTRACT

Brackish water desalination is a key solution for addressing the growing demand for drinking water in areas with limited access to freshwater resources. In this experimental study, reverse osmosis (RO), nanofiltration (NF), and single-pass electrodialysis (SPED) autonomous small-scale systems were investigated for brackish water desalination based on salt removal, specific energy consumption (SEC), and thermodynamic energy efficiency. With a production capacity of 40–180 L/h at a common recovery of 30 %, RO could achieve permeate salinities < 1000 mg/L at feed salinities up to 12 g/L, whereas NF and SPED were limited to 10 and 6 g/L, respectively. Under typical operation, defined here by 10 % recovery for a single NF/RO module and 50 % for a SPED system, permeate quality with salinity below 1000 mg/L could be achieved at ≤ 17.5 g/L for RO, and ≤ 15 g/L for NF and SPED. When operating at comparable recovery (30 %), SPED demonstrated lower SEC (0.7–1.4 Wh/L) than NF (1.8–3.2 Wh/L) and RO (2.4–3.7 Wh/L) across the investigated salinities 1–12 g/L. However, operating NF/RO at 10 % doubled the SEC due to reduced permeate production, while SPED maintained a stable SEC under 50 % recovery. For brackish water up to 12 g/L salinity, SPED showed higher energy efficiency than NF and RO when comparing experimental SEC with the minimum energy for desalination. These findings highlight the potential of SPED for low-to-moderate salinity brackish water, the suitability of NF/RO for stricter water quality, and the need for optimized recovery or hybrid processes to balance energy use and performance.

* Corresponding author.
E-mail addresses: youssef-amine.boussouga@um6p.ma (Y.-A. Boussouga), Andrea.Iris.Schaefer@kit.edu (A.I. Schäfer).
[1] Current address: International Water Research Institute (IWRI), University Mohammed VI Polytechnic (UM6P), Benguerir, Morocco.

https://doi.org/10.1016/j.desal.2025.119670
Received 6 October 2025; Received in revised form 4 November 2025; Accepted 19 November 2025
Available online 20 November 2025

1. Introduction

Four billion people live in areas that suffer from severe physical water scarcity [1]. This figure may increase to nearly 6 billion people by 2050 [2]. Water scarcity is a complex dynamic driven by multiple factors, including world population growth, climate change, and wasteful water management systems [3]. Lack of financial means to invest in water-supply infrastructure, especially in developing countries, is an additional challenge [4]. As freshwater remains essential for sustaining human activities [5], population growth and socio-economic development are anticipated to increase freshwater demand by 50–80 % over the next three decades [6,7]. At the same time, climate change influences global freshwater availability due to changes in seasonal precipitation, hence surface water and groundwater recharge [8–10]. In light of these challenges, desalination technologies are increasingly viewed as vital solutions. However, they risk transforming water scarcity into an energy problem if not managed properly [11]. Therefore, energy-efficient desalination methods are crucial to sustainably support the water-energy-food nexus [12].

1.1. Brackish water desalination

Desalination of seawater and brackish water can increase the availability while maintaining the freshwater cycle [13], and extending drinking water supplies [14]. Technically, seawater desalination is considerably more energy-intensive than brackish water desalination, owing to the higher salinity of seawater, which substantially increases the energy required for the desalination process [15]. Yet, brackish water is less explored and augmented by variable water composition, technological adaptation, and brine disposal logistics [16]. Globally, the total volume of brackish groundwater (12.9 million km^3) represents 55 % of the total volume of groundwater (23.4 million km^3) [17]. This distribution of brackish groundwater is further exacerbated by seawater intrusion and over-extraction of fresh groundwater [18]. Desalination of brackish groundwater, given its typically salinity of 1–10 g/L, has the potential to meet the growing water demand, particularly in dry inland regions [19]. Nevertheless, the water desalination industry market share is 21 % brackish water desalination compared to 61 % seawater desalination, with the remaining 18 % distributed across wastewater desalination and other industrial applications [20].

1.2. Brackish water membrane desalination technologies

In terms of technology, reverse osmosis (RO) is the dominant technology in global desalination – accounting for 86 % (65.5 million m^3/day) of total production across both seawater and brackish water desalination – followed by nanofiltration (NF) (3 % with 2.8 million m^3/day desalination capacity), and electrodialysis (ED) (2 % with 1.9 million m^3/day desalination capacity) [20]. Within these capacities, 27 % of RO and 60 % of ED desalination capacities are used for brackish water desalination [20], reflecting the fact that ED dominates brackish water desalination, while NF plays a minor role.

Despite ED being claimed to consume less energy than RO at low salinity ($\leq$ 5 g/L TDS) [21,22], RO is more commonly used in small-scale systems for brackish water desalination [23]. This could be due to the market size difference or likely due to the maturity of the technology, rather than actual performance. NF is less common for brackish water desalination, although it can provide comparable performance to low-pressure RO membranes, particularly for low salinity brackish water [24], and can be used in a hybrid process with RO to increase recovery [25], or improve the mineral composition of the permeate [26].

From an operational perspective, NF/RO and ED differ fundamentally in their driving forces. NF/RO require a pressure to drive water through to the permeate, while the solutes are retained in the concentrate. In ED, an electrical potential is applied across a stack of cationic and anionic exchange membranes, transporting ions to the concentrate and obtaining a diluate stream [27]. In semipermeable NF/RO membranes, the water-salt selectivity originates from the subnanometer-scale voids between polymer chains that enhance transport of water molecules (of a radius of about 1.3 Å) compared to hydrated ions (*e.g.* Na^+ 3.6 Å and Cl^- 3.3 Å [28]) [29]. In NF/RO, a critical energy barrier facing water molecules before being able to permeate through the subnanometer-scale voids is dependent on the membrane characteristics (pore size/volume and salt concentration) and the bulk osmotic pressure that controls the driving force for separation [30–32]. In NF, the non-steric interactions, including the electrostatic interactions of ions with the charged groups of the membrane material and the energy barriers associated with the partial dehydration of ions, play an important role in water-salt separation [33]. In contrast, in ED, semipermeable ion exchange membranes (IEM) – that include a polymeric matrix, ionic groups fixed in the matrix, and mobile ions in the interstices – favour the transport of ions between two solutions, resulting in diluted and concentrated streams [34]. Unlike NF/RO, water transport through the IEM is undesirable, and it can damage and reduce the lifecycle of the membrane [35]. Water transport in IEM is associated with hydrostatic pressure difference, the osmotic pressure difference, electro-osmosis due to ion-water friction, and the transport of hydrated ions [36]. In IEM, ions are selectively transported depending on the ionic charge, the operational conditions (such as applied current, water flow rate), the membrane characteristics (such as thickness, fixed charge density), and the water matrix [37,38]. Increasing salinity in ED results in more ions transported through the membranes; hence, more energy is required, and the selectivity of bivalent ions is reduced in favour of the dominant monovalent ions, such as Na^+ and Cl^- [39,40].

1.3. Renewable energy-powered small-scale ED and NF/RO systems

All desalination methods are known to be energy-intensive, and a significant amount of carbon dioxide is emitted from brackish water RO desalination plants (0.4–2.5 kg CO_2eq/m^3 [41,42]). To address this challenge and break out of the water-energy nexus paradigm, using a more renewable (sustainable) source of energy can offset such emissions. In particular, photovoltaic (PV)-powered desalination systems are at or nearing commercial scale [43]. Small-scale PV-powered NF/RO systems have been extensively tested for brackish water desalination [23], and can tolerate intermittency when operated directly from the solar resource (without any energy storage) [44]. Similarly, PV-powered ED systems have been deployed and operated at a small scale for brackish water desalination, both with different configurations (batch and continuous operations) and with/without an energy storage strategy [45,46].

1.4. Energy consumption of brackish water desalination with NF/RO and ED

In NF, RO, and ED, energy consumption remains an issue along with environmental impacts [47]. Therefore, reducing the specific energy consumption (SEC) for such technologies is a long-standing goal [48]. The SEC is commonly reduced in desalination plants when upscaling, due to smaller losses, maximising throughput, adopting hybrid processes, and improving operation and maintenance practices [21,49].

For NF/RO, SEC can be reduced by using membranes with higher selectivity-permeability trade-off [50–52], adopting low-pressure isobaric energy recovery devices [53], considering multi-stage approaches in the process [54,55], and using active-salinity-control for dynamic power consumption [56]. Similarly, in ED, SEC can be lowered by using low electrical resistance membranes with better system designs, such as in the case of adopting using thinner spacer [57,58], optimizing the operating conditions, such as current density, temperature, and flow rate [39,40,59], and implementing advanced control strategies to help optimize ED performance [60].

The SEC of electrically-powered desalination processes (NF, RO, and

ED in this case) depends on i) either *via* the use of electricity to drive a high-pressure pump (NF/RO) or systems that rely on direct current (DC) electricity directly to realise desalination (ED), ii) feedwater salinity, and iii) the production capacity of the system [61]. Fig. 1 shows the dependence of SEC in NF/RO and ED on salinity at different system capacities as reported in the literature. The main observations are that i) SEC increases with salinity, ii) SEC decreases with scale, and iii) SEC of ED appears lower than that of NF/RO. System design, operating conditions, and membrane choice will clearly affect these results. Increasing salinity requires more pressure to overcome the osmotic pressure in NF and RO operation, which results in higher SEC. This is typical behaviour in NF and RO systems [62]. In ED, higher salinity results in higher ion transport and hence current, resulting in a higher SEC (due to diminishing current efficiency) [63].

Inevitably, system capacity plays a key role. In RO, increasing system size generally reduces SEC because larger pump stations achieve greater efficiency [62]. In contrast, in ED, SEC at a given (*e.g.,* 5 g/L) tends to increase with capacity because the current efficiency in ED is strongly related to productivity, being greatly enhanced by larger current densities [63]. Additionally, pumping the different streams is required for ED operation, and this can make a significant contribution to the overall SEC, particularly for small-scale systems [64].

Improving the energy efficiency of NF/RO and ED desalination processes – by reducing the SEC toward the theoretical absolute minimum amount of energy required for water-salt separation – is essential for the sustainability of desalination technologies, as it helps lower both operating costs and the carbon footprint.

1.5. Thermodynamic minimum energy requirements of desalination

The thermodynamic limit – defined as the difference between the Gibbs free energy of the mixture (water and salt in this case) and the Gibbs free energy of each component – is based on the second law of thermodynamics of real processes involving entropy generation (loss of energy) [65,66]. Approaching this thermodynamic limit represents achieving the minimum specific energy consumption (SEC_{min}) required for salt-water separation (regardless of the process) [67], and minimizing the energy barriers of water transport in NF/RO and selective ion transport in ED must be targeted.

The SEC_{min} for seawater RO desalination operating at 50 % recovery with a feed salinity of 35 g/L is approximately 1.14 Wh/L [48]. The state-of-the-art seawater RO desalination with 50 % recovery exhibits ~3 Wh/L [53], which is equivalent to ~31 % energy efficiency. With ED, this can be achieved by a multi-stage configuration exhibiting 3 Wh/L at 40 % water recovery [68,69]. Applying the same calculation approach as Wang et al. [48], the SEC_{min} for brackish water desalination with a salinity range of 1–20 g/L varies between 0.03 and 0.65 Wh/L at 50 % water recovery. Increasing the water recovery results in increased SEC_{min} [70].

Given the wide variability in brackish water quality and the scalability of different desalination technologies, there remains a lack of consistent experimental data directly comparing NF, RO, and ED under controlled and comparable conditions. Such a comparison is essential to accurately evaluate the energy efficiency of brackish water desalination under realistic operating scenarios. When comparing the technologies, the specific research questions to be addressed are: (i) what is the SEC of ED *versus* NF/RO as a function of salinity?, (ii) how does the SEC of ED and NF/RO compare to SEC_{min} as a function of salinity?, and (iii) to what extent does the typical recovery used for small-scale NF/RO and ED systems affect the process performance, in terms of salt removal and energy consumption? The outcomes of this study provide experimental evidence clarifying how salinity and recovery influence the energy efficiency of the investigated brackish water desalination technologies. The findings contribute to a more robust understanding of process selection for energy-efficient brackish water desalination.

2. Materials and methods

A description of the small-scale NF/RO and ED systems, both designed to be coupled with PV panels in a mobile system, is presented, with a particular focus on the limitations that arise when comparing these technologies at the same recovery of 30 % and during operation at typical recoveries based on the actual system scale, 10 % for NF/RO and 50 % for ED.

2.1. Nanofiltration/reverse osmosis system

A small-scale NF/RO system, built in-house, was used, which consists of a membrane system NF/RO with a pre-treatment step using ultrafiltration (UF) and system control. A system schematic is shown in Fig. 2A. The system has a customized feed tank (RDM Producten, The Netherlands) with external dimensions (l × w × h) of 1.4 × 0.5 × 0.7 m (490 L), and two stainless steel pressure vessels (PVS 4040 rated at 41.4 bar, Inaqua, Germany), housing a 4" NF/RO module and a UF membrane module. The 4" NF/RO membranes had an active filtration area of 7.6 m^2 and were selected based on the high salt rejection characteristics at relatively high flux, suitable for brackish water desalination – either NF90 (NF membrane) and BW30 (RO membrane), both supplied from DuPont (Germany). The properties of the membranes are summarised in **Table S2**.

An UF membrane with multibore structure made of polyethersulfone (PES) with an active filtration area of 6.0 m^2 and pore size of 20 nm

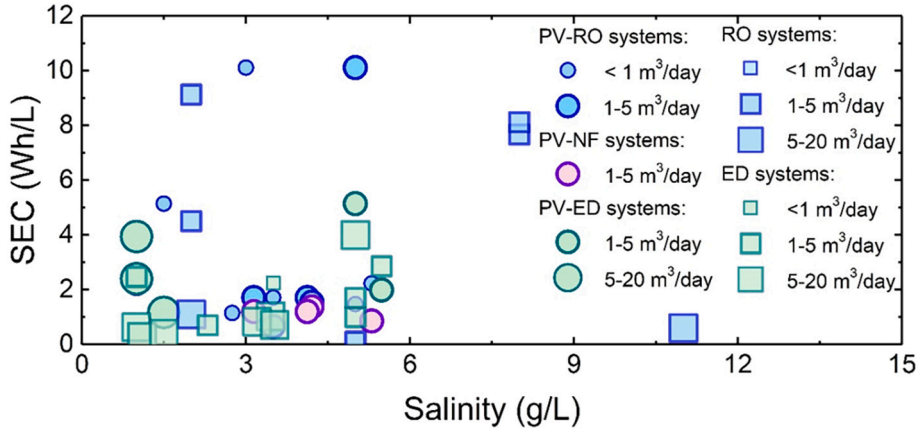

Fig. 1. Experimental SEC values for NF/RO and ED desalination systems from the literature – some powered with PV – as a function of salinity. The systems are classified into small (<1 m^3/day), medium (1–5 m^3/day), and large (5–20 m^3/day). The data points, along with the references, are provided in **Table S1**.

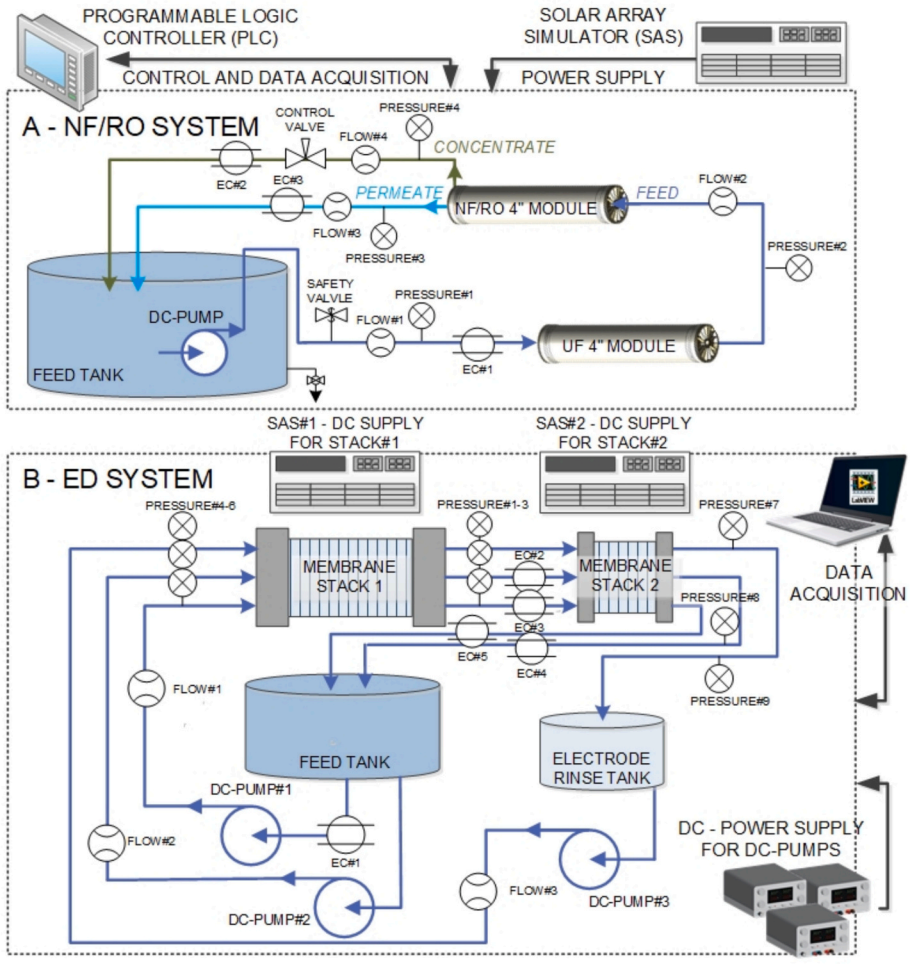

Fig. 2. Schematic flow diagram of (A) the NF/RO and (B) the ED systems, showing the main system components, pump(s), UF membrane, NF/RO membrane for the NF/RO system, and membrane stacks for the ED system. The data acquisition system is connected to a computer running LabVIEW for ED, while the PLC is used for the NF/RO system. EC denotes electrical conductivity.

(Dizzer P4040–6.0, Inge-DuPont, Germany) was used for pre-treatment and to protect the NF/RO membranes.

The system performance and operation can be monitored and controlled using a programmable logic controller (PLC, Unistream 10.4″, Unitronics, Israel), enabling process visualisation, real-time data processing, and control for up to 32 analog inputs (4-20 mA or 0-10 V). Through the expansion modules, 16 digital outputs were integrated, which allows the control of the relays and actuator valve control in the system setup. For monitoring system operation, high-pressure flow sensors (Promag H300 5H3B08-MJL4/0, Endress Hauser, Switzerland) for feed and concentrate flowrate, bi-directional flow sensor (MIM-1203HG4C3TO, Kobold, Germany) for permeate flowrate with a minimum electrical conductivity (EC) requirement of 20 µS/cm that measure pressure relative to atmospheric pressure, and pressure sensors (Type 8316, Bürket, Germany) for feed and concentrate pressures. For back pressure control, an actuator-driven valve (MCM-S50AF-3-SS-18RF8, Hanbay, USA) in the concentrate stream and connected to the PLC is used. For water quality monitoring, high-pressure EC sensors for feed and concentrate (Type 4221, Valmet, Finland), EC sensor (Type 8222, Bürket, Germany) for NF/RO permeate, a high-pressure pH sensor (3300HTVP-10-30, Emerson, USA) for feed, and pH sensor (Type 8202, Bürket, Germany) for NF/RO permeate are installed in the system.

In terms of power supply options, the system is designed to be (i) coupled with a solar array simulator (SAS) (62050H- 600S, 0–600 V, 0–8.5 A, Chroma, Taiwan), a 5 kW-rated programmable DC power supply that enables the simulation of real-world solar panel characteristics, solar irradiance (SI), and temperature for laboratory experiments, and (ii) connected to PV panels in a mobile system using a trailer. In this work, the SAS was used to simulate the output of silicon PV panels (Offgridtec 100 W, 39.6 V, Offgridtec GmbH, Germany) under standard test conditions, with a fixed solar irradiance of 1000 W/m^2 and a cell temperature of 25 °C, to generate a constant maximum power output. The configuration was arranged in three series-connected and two parallel-connected modules, achieving a total power of 600 W (P_{mp}) with corresponding parameters of $V_{mp} = 118.8$ V and $I_{mp} = 5.89$ A. Two different helical rotor pumps – Grundfos SQFlex0.6-2 N ($P_{max} = 420$ W; 1–12 bars) and Grundfos SQFlex0.6-3 N ($P_{max} = 580$ W; 8–20 bars) – were used to overlap the required pressure for the treatment of salinity from 1 to 20 g/L, corresponding to an osmotic pressure (π) range of 0.9–17.8 bar. The pump curve characteristics of these two pumps are shown in **Fig. S1**. The pumps can operate at a DC voltage within the range of 30–300 V, and can generate a maximum feed flow rate (Q_f) of 600 L/h (at 20 bar maximum with Sqflex0.6-3 N) and (at 12 bar maximum with Sqflex0.6-2 N).

Given the focus of this work is to investigate the system performance at fixed recovery rates, the fixed recovery setpoint method was adopted. This is contrary to the constant power set-point strategy, adopted in the previous works [71,72]. The constant recovery setpoint control strategy

maintains a consistent recovery rate of permeate regardless of varying feed water quality. For this, the pumps were allowed to draw up to the maximum power that could be supplied by the SAS (emulating the 420 W for SQFlex0.6-2 N and 580 W for SQFlex0.632 N supply from the PV), hence a fixed feed flow rate ($Q_f \sim 600$ L/h), while the back pressure control valve was adjusted until the required permeate flow rate (Q_p) defined the controlled recovery. The system was kept running for 15 min to allow the readings to be at a steady state before data acquisition was carried out.

2.2. Electrodialysis system

A single-pass ED system (Deukum GmbH, Germany) for treating brackish water was employed with a maximum production of 100 L/h (Fig. 2B). The system is composed of two rectangular tanks for electrode rinse (35 L) and feed (85 L) solutions, and equipped with cationic (FKS-130, Fumatech, Germany) and anionic (FAS-130, Fumatech, Germany) ion-exchange membranes in two stacks (TYPE 1800, Deukem GmbH, Germany) in series for continuous operation. The first stack has 30 cell pairs (total area 10.8 m^2) while the second has 15 cell pairs (total area 5.4 m^2) of membranes. This is comparable in membrane area to two 4" NF/RO modules (7.6 m^2 each). Three brushless-DC magnetic pumps (GRI PUMPS INTG3–70, USA) are used for pumping diluate, concentrate, and electrode rinse solutions through the membrane stacks. The diluate pump is powered by a variable DC power supply (VOLTCRAFT DPPS 32–15 DC, Germany), while two variable DC power supplies (BASETECH BT-305, Germany) are used for the concentrate and electrode rinse pumps.

To simulate the DC power supply from the PV panels to the ED stacks, one SAS (62020H—150S, 0–150 V; 0–40 A, Chroma, Taiwan) was used per stack. The maximum potential needed for the ED membrane stacks is 1 V/cell pair [73], while the maximum current depends on the salinity of the feedwater. At each stage, the applied electric potential can be adapted to the feed salinity and can then be operated at its optimum condition to achieve highest removal and lowest energy consumption. The potential required to drive the ED system was set based on the limiting current density (LCD), which determines the optimum potential to achieve high removal and protect the stacked membranes, required for each stack based on the feed salinity. This means that each stack of the ED system was working at the LCD, which was determined by the polarization curve [74]. The LCD results can be seen in **Fig. S3** for the 30 % recovery and **Fig. S4** for the 50 % recovery. For system performance monitoring, sensors are used to measure pressure (PU5415, ifm electronic, Germany), flow rate (SM4100, ifm electronic, Germany), and EC (CR-GT and CR-EC, JUMO, Germany). The signals emitted by the sensors are read by the software LabView (v2018, National Instruments, USA) through a data acquisition (DAQ) card (USB-6218, National Instruments, USA).

2.3. System operation at variable water recovery

For NF/RO experiments, the system was operated at 10 % and 30 % recovery. With a fixed Q_f of 600 L/h, the 10 % recovery corresponded to Q_p of 60 L/h and flux of 8 L/m^2.h, while 30 % corresponded to Q_p of 180 L/h and flux of 24 L/m^2.h. The selected recoveries for NF/RO were based on the worst-case scenario, which is BW30 of low water permeability operated at a maximum pressure of 20 bars. For this reason, the investigations were limited to 12 g/L NaCl (corresponding to an osmotic pressure (π) of 10.0 bar at 22 °C) at 30 % recovery and 20 g/L NaCl (corresponding to π of 16.6 bar at 22 °C) at 10 % recovery. To validate the performance of the NF/RO system, the experiments at 10 % recovery were carried out in a different system of similar size and specifications. Details on the system design used for this comparison were previously published by Ogunniyi and Richards [75]. For ED experiments, the recovery was fixed at 30 % with a diluate flow rate (Q_d) of about 42 L/h and Q_f at 140 L/h. Further experiments were carried out at the maximum water productivity of the system according to the supplier (Q_d 100 L/h), which corresponded to a recovery of 50 %. Performance parameters relevant to NF/RO system operation, such as transmembrane pressure (TMP) and water flux, and to ED system operation, such as current density, in addition to salt removal, solute flux, SEC, and energy efficiency, are summarised in **Table S3.** Error analysis was evaluated based on the absolute errors for the measured quantities and the calculated parameters using **Table S4**.

2.4. Solution chemistry

Feed solutions were freshly prepared with deionized (DI) water (EC < 1 µS/cm, pH 6.2 $\pm$ 0.4) and sodium chloride (NaCl, VWR chemicals, purity $\geq$99.9 %, Germany) at salinities varied from 1 g/L to 20 g/L, without the addition of bicarbonates. The selected NaCl concentrations (1–20 g/L NaCl; corresponding to an osmotic pressure (π) range of 0.8–16.6 bar at 22 °C) cover a wide range of brackish water salinities. The correlation between EC and NaCl concentrations of the feed solutions is shown in **Fig. S2**.

3. Results and Discussion

A comparative study was conducted to evaluate the desalinated water quality and energy consumption of small-scale desalination systems using NF, RO, and ED technologies. The energy efficiency was assessed relative to theoretical energy limits, emphasizing the impact of salinity, system size, and water recovery. To enable a fair comparison of NF, RO, and ED technologies, initial experiments were conducted at a uniform recovery of 30 %.

3.1. Desalination performance of single-pass NF/RO and ED systems at identical recovery

The small-scale NF, RO, and ED systems were evaluated to determine to what extent the target desalination of 1000 mg/L (WHO recommended upper limit for TDS based on palatability [76]) and the resulting driving forces (pressure for NF/RO and current for ED) when treating brackish water with salinity ranging from 1 to 12 g/L. All systems were operated at 30 % water recovery (Fig. 3). It should be noted that the experiments carried out at 30 % recovery were limited to 12 g/L salinity because of the pressure limitations of the NF/RO system (20 bar) to achieve a controlled permeate flow rate of 180 $\pm$ 20 L/h. The supplementary data on the stability of the operating and other water quality parameters are reported in **Figs. S5** and **S6** for NF/RO experiments and **Figs. S7** and **S8** for ED experiments, while mass balance evaluation is reported in **Fig. S9.**

As expected for NF and RO, the required TMP (at fixed recovery) increased with increasing salinity (Fig. 3A). Similarly, in the ED, the current density increased with salinity in both stacks (Fig. 3B), in which stack 2 exhibited a larger current since it received the desalinated water from stack 1. In terms of water quality, the WHO TDS recommendation for acceptable drinking water of <1000 mg/L was achieved with BW30 over the salinity range of 1–12 g/L. In contrast, NF performance was limited to salinities $\leq$10 g/L, whereas ED could only achieve the required water quality up to 6 g/L (Fig. 3C). The step observed with ED from 3 to 4 g/L was caused by the different applied potential, varied from 3 V at 3 g/L to 4 V at 4 g/L, to operate the ED system at the LCD of the stacks. The decrease of salinity removal with increasing NaCl concentration was expected for NF, RO, and ED due to concentration polarization, enhancing salt transport in NF/RO membranes [32], and ion exchange membranes [77].

Overall, at this stage, it is evident that the water quality achievable through brackish water desalination is constrained by both the feed water salinity and the choice of desalination technology (NF, RO, ED). The SEC associated with each technology is therefore assessed in the following section to better understand the trade-offs between water

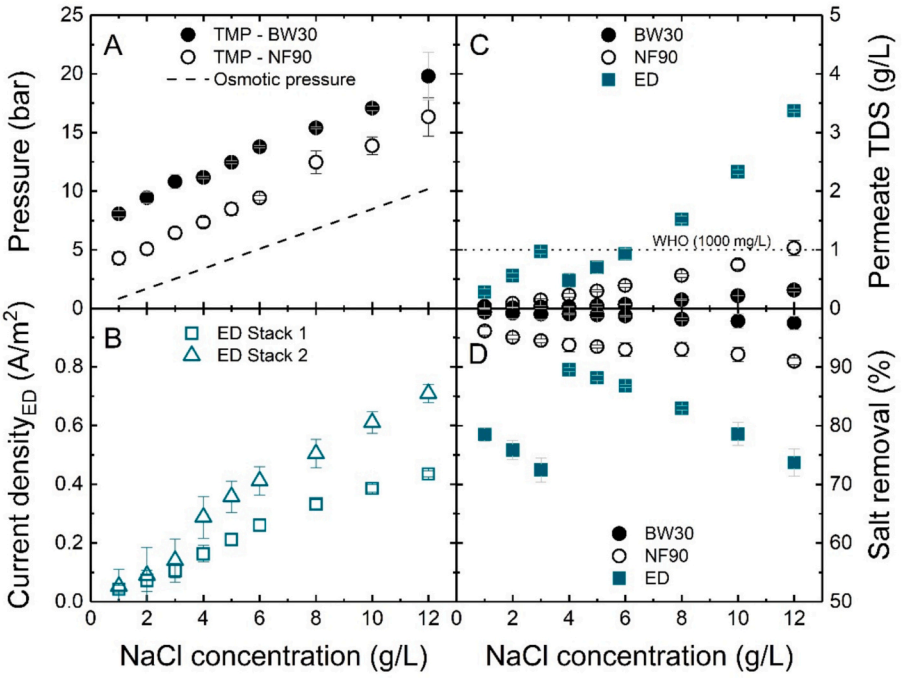

Fig. 3. Desalination performance parameters as a function of NaCl concentration: (A) NF/RO transmembrane pressure compared to the osmotic pressure of the feed water, (B) current density exhibited in the ED stacks, (C) permeate quality, and (D) salt removal comparison (30 % recovery, $Q_{p\text{-}NF/RO}$ 180 ± 20 L/h, $Q_{d\text{-}ED}$ 42 ± 2 L/h, $U_{stacks1–3\ g/L\ NaCl}$ 3 V, $U_{stacks\ 4–12\ g/L\ NaCl}$ 4 V).

quality and energy demand.

3.2. SEC comparison of NF/RO and ED for brackish water desalination at identical recovery

To evaluate the energy requirements of NF/RO and ED systems operated at different feed salinities, the power consumption and SEC were investigated over the salinity range of 1–12 g/L NaCl (Fig. 4).

The power consumed, either by the DC pump to drive NF and RO or the ED stacks, increased with NaCl concentration and reached a plateau for NF and RO in the range of 8–12 g/L NaCl (Fig. 4A). This plateau could be due to improved pump efficiency at higher pressures (**Fig. S1**), which restricts further increases in power demand at higher salinities. In contrast, in the ED system, the power consumed by the DC pumps used to generate flow rates in different streams was the major contributor to the total power consumption within the salinity range of 1–6 g/L, remaining constant at approximately 25 W (Fig. 4A). As a result, ED exhibited lower SEC, falling within the reported range for brackish water desalination by ED (0.4–4 Wh/L [78]), compared to NF and RO (Fig. 4B). This lower SEC can be explained by the fact that the power required for ED was ten times lower than that for NF and RO, while Q_d was only five times lower than Q_p.

Overall, the SEC comparison of NF, RO, and ED for brackish water desalination confirms that RO is the most energy-intensive, while ED is the least. However, at the investigated scale of the ED systems, the total SEC is still largely dominated by the power consumption of the stacks rather than the pumps. To further understand these energy demands in relation to theoretical energy demands, the energy efficiency of these processes was investigated in the following section using the principles of the thermodynamic limit.

3.3. Thermodynamic energy efficiency at different salinities

The thermodynamic energy efficiency (η) is defined as the ratio of

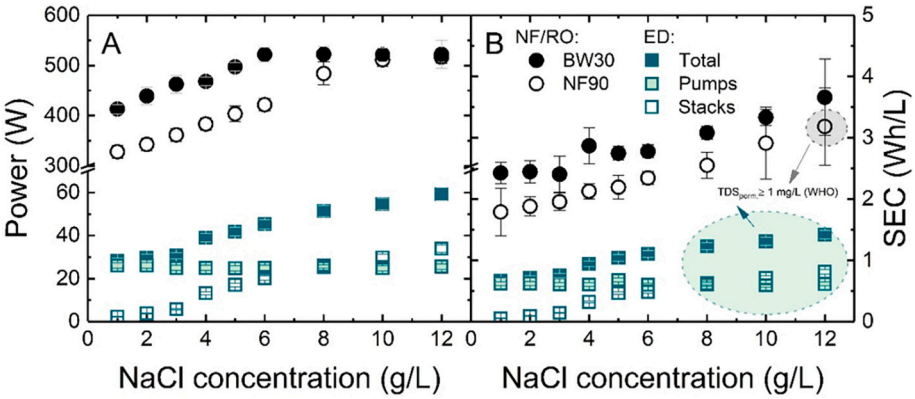

Fig. 4. (A) Power consumption and (B) SEC in ED (total, of the stacks and of the pumps) and NF/RO (pump) as a function of NaCl concentration. (30 % recovery, $Q_{p\text{-}NF/RO}$ 180 ± 20 L/h, $Q_{d\text{-}ED}$ 42 ± 2 L/h, $U_{stacks1–3\ g/L\ NaCl}$ 3 V, $U_{stacks\ 4–12\ g/L\ NaCl}$ 4 V).The shaded areas in (B) indicate the SEC values where the WHO target (< 1000 mg/L) was not achieved.

the SECmin for the chosen salinity and recovery to the measured experimental SEC for a particular system at the same salinity and recovery. To evaluate the energy efficiency of the three processes (NF, RO, and ED), the SECmin and η were calculated, based on the obtained experimental performance, and investigated over the NaCl concentration 1–12 g/L (Fig. 5). It should be noted that the reported η values lie well below 100 % due to practical constraints – including frictional losses in the systems, pump efficiency, membrane resistance to water and ion transport – which cannot be individually distinguished in the present experimental conditions.

The SEC_{min}, calculated based on the salt removal obtained experimentally from operating NF, RO, and ED systems, shows a clear linear increase with rising NaCl concentration from 1 to 12 g/L (**Fig. 5A**). This trend reflects the growing minimum energy demand required to remove higher salt loads from brackish water as salinity increases. When evaluating the (thermodynamic) energy efficiencies, RO and ED exhibit a wide range depending on salinity: η in RO varies between 2 and 20 %, while η in ED spans from 11 to 60 % (**Fig. 5B**). These values align well with reported literature ranges for similar salinities in the literature, where η in RO falls between 10 % and 45 %, and in ED efficiency between 4 % and 46 % at around 15 g/L NaCl [70]. Notably, ED consistently outperforms NF and RO in terms of energy efficiency, particularly at lower salinities (1–6 g/L), where it successfully meets the WHO recommendation. This is largely attributed to the low experimental SEC values observed for ED under these conditions.

To ensure a fair comparison of NF, RO, and ED, the previous experiments were carried out at the same recovery of 30 %, which is above the design specifications of one 4" NF/RO module (≤15 % to achieve ≤24 L/m^2.h for desalination [79]). Exceeding this recommended limit for one 4" NF/RO module, especially for long-term operation, enhances the formation of scaling when dealing with natural brackish water, and hence reduces the module lifetime due to regular cleaning requirements [80]. NF/RO systems can operate at recoveries ≥30 % for brackish water desalination by adding more modules and meeting the increased electrical pumping requirements [81]. Small-scale ED systems, on the other hand, can be operated at higher recoveries (50–90 %) [45]. The following section evaluates the performance of NF, RO, and ED for brackish water desalination across salinities ranging from 1 to 20 g/L, using a more representative recovery to practical applications: 10 % for NF and RO, and 50 % for ED.

3.4. Performance of single-pass NF/RO and ED at typical recovery

The performance, in terms of driving forces, salt removal, and energy requirement, of NF, RO, and ED is typically affected when varying the recovery of the process. For this, the small-scale NF, RO, and ED systems were operated at typical recovery conditions (10 % for NF/RO and 50 % for ED) to desalinate feed waters with 1–20 g/L salinities and compared to the results obtained at 30 % recovery (Fig. 6). Supplementary data on operating parameters and water quality are reported in **Figs. S9-S12**.

The required TMP for operating NF and RO decreased when adopting low recovery (10 %) (Fig. 6A), which is attributed to the reduced flux produced under these conditions (Fig. 6D). In contrast, for ED, the required current density increased in both stacks when operating at a higher recovery of 50 % (Fig. 6B), reflecting the greater driving force needed for ion transport at elevated recovery. Regarding water quality, the WHO recommendation (<1000 mg/L TDS) was achieved with BW30 at salinities up to 17.5 g/L, while NF90 met this standard only at salinities ≤15 g/L (Fig. 6C). The quality of permeate was better in 10 % recovery than in 30 % recovery for NF and RO, due to low solute flux (Fig. 6F). This improved quality at lower recovery (10 %) is likely due to reduced concentration polarization (CP), resulting in enhanced salt removal efficiency (Fig. 6E). In the case of ED, increasing the recovery from 30 % to 50 % led to improved permeate quality, with the WHO recommendation achieved at salinities ≤15 g/L (Fig. 6C). This improvement corresponds to the increase in salt removal (Fig. 6E), and can be attributed to the higher current density applied to drive ion migration through the membranes.

To elucidate the energy consumption at different recoveries, the SEC was determined for the experiments at 10 % recovery for NF and RO and 50 % recovery for ED. For this, the SEC was investigated over NaCl concentrations of 1–20 g/L (Fig. 7).

When operating the NF/RO system at 10 % recovery and ultimately lower flux, the pump required less power due to the reduced TMP necessary for operation (Fig. 7A). In the case of ED, the low power demand observed at 30 % recovery, particularly at salinities of 8–12 g/L, is attributed to the low current density applied to drive the ED stacks (Fig. 7A).

The SEC for ED did not change much when the recovery was increased from 30 to 50 %, especially at salinities 1–8 g/L (Fig. 7B). This stability can be explained by the similar current density applied in both recovery settings within this range. At 10 % recovery, NF and RO exhibited a significant increase in SEC (Fig. 7B). This rise in energy consumption is linked to the low permeate production (Q_p 60 L/h) compared to operation at 30 % recovery (Q_p 180 L/h). Similar findings have been reported for other small-scale NF/RO systems for brackish water desalination when comparing performance across different recoveries [82,83].

These results highlight the strong influence of the system scale on the energy performance of desalination technologies. While lower recovery can improve water quality by reducing CP and TMP, it also led to higher SEC for NF and RO due to reduced permeate production. In contrast, ED remains less sensitive to recovery changes within the studied salinity range, maintaining stable SEC values. Therefore, optimizing recovery is

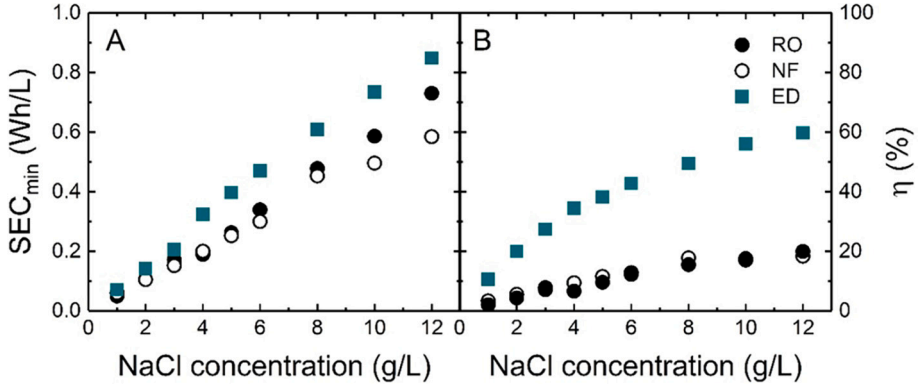

Fig. 5. (A) theoretical minimum SEC (SEC_{min}) and (B) energy efficiency (η) in ED (for stacks with pumps) and NF/RO (pump) as a function of NaCl concentration (30 % recovery, $T_{NF/RO}$ 20–29 °C, T_{ED} 22 ± 1 °C, $Q_{p\text{-}NF/RO}$ 180 ± 20 L/h, $Q_{d\text{-}ED}$ 42 ± 2 L/h, $U_{stacks1–3\ g/L\ NaCl}$ 3 V, $U_{stacks\ 4–12\ g/L\ NaCl}$ 4 V).

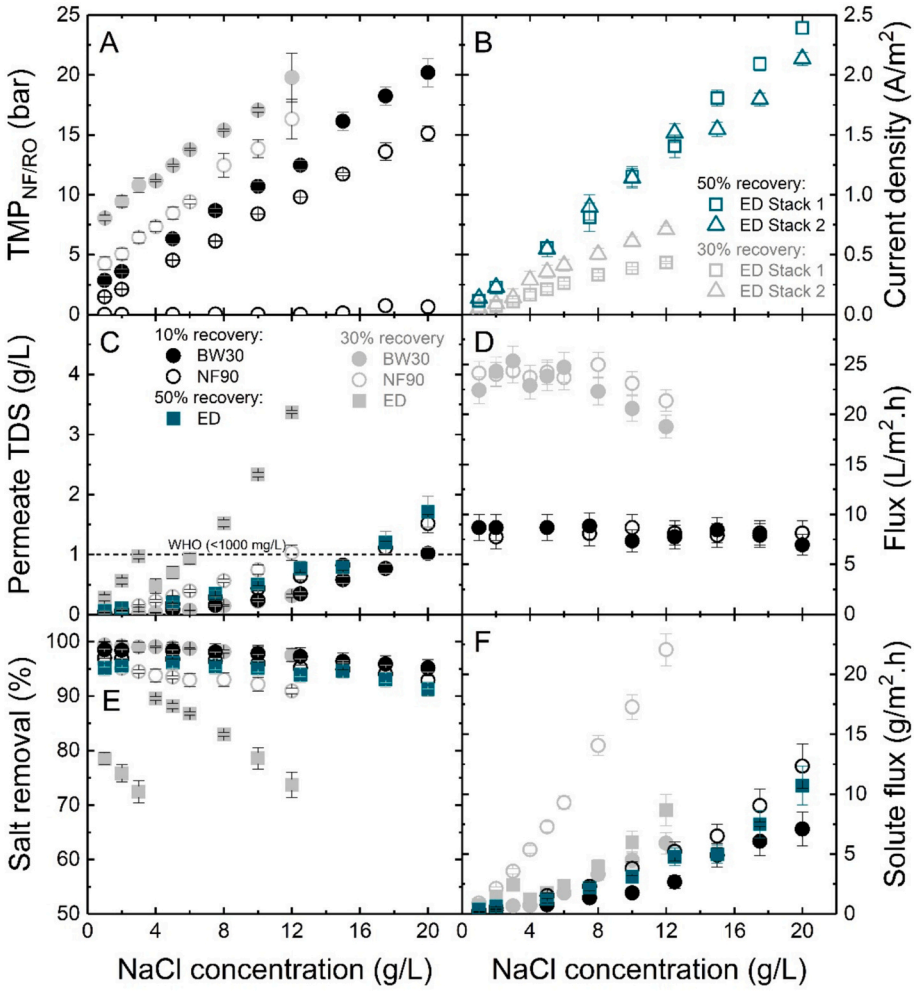

Fig. 6. Desalination performance parameters as a function of NaCl concentration: (A) NF/RO transmembrane pressure, (B) current density exhibited in the ED stacks, (C) permeate quality, and (D) NF/RO flux, (E) salt removal, and (F) solute flux (NF/RO: Q_p 60 L/h, 10 % recovery; ED: 50 % recovery, Q_d 100 L/h, $U_{stacks1,2,\ 1–2\ g/L\ NaCl}$ 6 V, $U_{stack2,\ 5–20\ g/L\ NaCl}$ 7 V, $U_{stack1,\ 5–7.5\ g/L\ NaCl}$ 7 V, $U_{stack1,\ 10–12.5\ g/L\ NaCl}$ 8 V, $U_{stack1,\ 15–20\ g/L\ NaCl}$ 10 V; T 22 ± 1 °C). The data points in grey are from Fig. 3 for comparison.

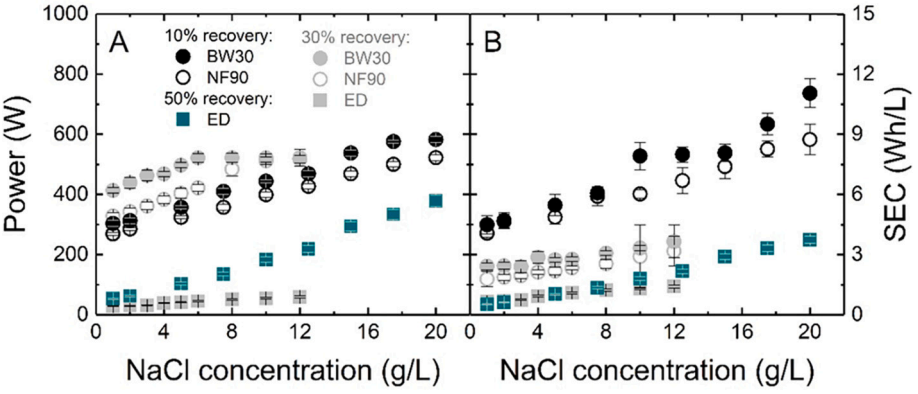

Fig. 7. (A) Power consumption and (B) SEC in ED (for stacks with pumps) and NF/RO (pump) as a function of NaCl concentration. (NF/RO: Q_p 60 L/h, 10 % recovery; ED: 50 % recovery, Q_d 100 L/h, $U_{stacks1,2,\ 1–2\ g/L\ NaCl}$ 6 V, $U_{stack2,\ 5–20\ g/L\ NaCl}$ 7 V, $U_{stack1,\ 5–7.5\ g/L\ NaCl}$ 7 V, $U_{stack1,\ 10–12.5\ g/L\ NaCl}$ 8 V, $U_{stack1,\ 15–20\ g/L\ NaCl}$ 10 V; T 22 ± 1 °C). The data points in grey are from Fig. 4 for comparison.

crucial for balancing water quality targets with energy efficiency, and the choice of technology must consider the interplay between salinity, recovery, and energy demands. In addition to salinity, real brackish water contains multivalent ions such as Ca^{2+}, Mg^{2+}, and SO_4^{2-}, which increase scaling tendencies in NF/RO systems, resulting in higher hydraulic resistance and thus elevated SEC [84]. Similarly, in ED systems, multivalent ions can reduce ion mobility and current efficiency [39,40]. As a result, the overall energy efficiency could be reduced compared to membrane processes treating feed solutions containing NaCl only. While this study intentionally used simplified feed

compositions to isolate the impact of salinity on SEC, future investigations using real brackish water matrices would be valuable to quantify the influence of multivalent ions on both performance and long-term operational stability.

4. Conclusions

A side-by-side comparison for desalination and energy efficiency, elucidated from the theoretical and experimental SEC, of NF, RO, and ED processes, was conducted for brackish water desalination. At a controlled recovery of 30 %, RO was the most effective in meeting the WHO guideline of 1000 mg/L TDS across the investigated salinity range (1–12 g/L), but it exhibited the highest SEC (2.4–3.7 Wh/L) compared to NF (1.8–3.2 Wh/L) and ED (0.7–1.4 Wh/L). Analysis of the experimental SEC relative to the minimum SEC revealed that ED achieved the highest energetic efficiency (up to 60 %), outperforming NF and RO, though it remained limited to low-salinity brackish water (1–6 g/L). When operated under typical recovery conditions dictated by system design—10 % for a single 4" NF/RO module and 50 % for a single-pass ED system—SEC increased notably for NF and RO due to reduced permeate production, whereas ED maintained stable SEC and achieved superior salt removal.

These results highlight the trade-offs between energy consumption, recovery, and water quality, underlining the potential of ED for low-salinity brackish water desalination and the suitability of NF/RO for achieving stricter water quality targets despite higher energy demands. Future work on such small-scale NF/RO and ED systems ought to focus on optimizing strategies for long-term operation and exploring hybrid configurations to balance energy efficiency and water quality across a broader salinity range.

CRediT authorship contribution statement

Youssef-Amine Boussouga: Writing – review & editing, Writing – original draft, Visualization, Validation, Supervision, Project administration, Methodology, Investigation, Formal analysis, Data curation, Conceptualization. **Ramatisa Ladeia Ramos:** Writing – review & editing, Validation, Supervision, Methodology, Investigation, Data curation. **Emmanuel O. Ogunniyi:** Writing – review & editing, Software, Methodology, Investigation, Data curation. **Bryce S. Richards:** Writing – review & editing, Supervision, Methodology, Funding acquisition, Conceptualization. **Andrea I. Schäfer:** Writing – review & editing, Supervision, Funding acquisition, Conceptualization.

Declaration of competing interest

The authors declare that they have no known competing financial interests or personal relationships that could have appeared to influence the work reported in this paper.

Acknowledgements

The Helmholtz Association is acknowledged for providing research funding for AIS (IAMT) and BSR (IMT) through the Recruitment Initiative, as well as for Research Field Energy – Materials and Technologies for the Energy Transition program (Topic 1 Photovoltaics and Wind Energy, 38.01.04). The BMBF project CEWAG (project number 03SF0575) is acknowledged for the partial funding of the photovoltaic-powered membrane system construction. DuPont Water Solutions are thanked for providing the NF/RO (former Dow FilmTech), and UF (former Inge) membrane modules, and Deukum GmbH for their assistance with system design and sensor integration. DAAD funding for the scholarships of Ramatisa Ladeia Ramos and Emmanuel Ogunniyi is gratefully acknowledged. Francis Adu-Boahene and Yike Meng are acknowledged for repeating the ED experiments at 30 % recovery, and Laura Alvarez is acknowledged for repeating the NF/RO experiments at 30 % recovery.

Appendix A. Supplementary data

Supplementary data related to this article are available in the Supporting Information (SI) section. The SI includes additional figures and comments covering: (i) reported SEC values in the literature for small-scale NF, RO, and ED systems for brackish water desalination; (ii) membrane characteristics; (iii) pump performance curves used in NF/RO operation; (iv) data and error analysis; (v) electrical conductivity measurements for different NaCl concentrations; (vi) determination of the limiting current density in ED experiments; (vii) supplementary NF, RO, and ED experimental results at 30 % recovery; and (viii) supplementary data on NF/RO at 10% recovery and ED at 50% recovery. Supplementary data to this article can be found online at https://doi.org/10.1016/j.desal.2025.119670.

Data availability

Data will be made available on request.

References

[1] M. Mekonnen Mesfin, Y. Hoekstra Arjen, Four billion people facing severe water scarcity, Science Advances 2 (2016) e1500323.
[2] U. WWDR, The United Nations World Water Development Report 2020: Water and Climate Change, UNESCO, 2020.
[3] F. Dolan, J. Lamontagne, R. Link, M. Hejazi, P. Reed, J. Edmonds, Evaluating the economic impact of water scarcity in a changing world, Nat. Commun. 12 (2021) 1915.
[4] R. Emile, J.R. Clammer, P. Jayaswal, P. Sharma, Addressing water scarcity in developing country contexts: a socio-cultural approach, Humanities and Social Sciences Communications 9 (2022) 144.
[5] T.M. Lenton, C. Xu, J.F. Abrams, A. Ghadiali, S. Loriani, B. Sakschewski, C. Zimm, K.L. Ebi, R.R. Dunn, J.-C. Svenning, M. Scheffer, Quantifying the human cost of global warming, Nat. Sustainability 6 (2023) 1237–1247.
[6] P. Greve, T. Kahil, J. Mochizuki, T. Schinko, Y. Satoh, P. Burek, G. Fischer, S. Tramberend, R. Burtscher, S. Langan, Y. Wada, Global assessment of water challenges under uncertainty in water scarcity projections, Nat. Sustainability 1 (2018) 486–494.
[7] D. Garrick, L. De Stefano, W. Yu, I. Jorgensen, E. O'Donnell, L. Turley, I. Aguilar-Barajas, X. Dai, R. de Souza Leão, B. Punjabi, B. Schreiner, J. Svensson, C. Wight, Rural water for thirsty cities: a systematic review of water reallocation from rural to urban regions, Environ. Res. Lett. 14 (2019) 043003.
[8] X. Kuang, J. Liu, B.R. Scanlon, J.J. Jiao, S. Jasechko, M. Lancia, B.K. Biskaborn, Y. Wada, H. Li, Z. Zeng, Z. Guo, Y. Yao, T. Gleeson, J.-P. Nicot, X. Luo, Y. Zou, C. Zheng, The changing nature of groundwater in the global water cycle, Science 383 (2024) eadf0630.
[9] S. Jasechko, H. Seybold, D. Perrone, Y. Fan, M. Shamsudduha, R.G. Taylor, O. Fallatah, J.W. Kirchner, Rapid groundwater decline and some cases of recovery in aquifers globally, Nature 625 (2024) 715–721.
[10] G. Li, T.E. Törnqvist, S. Dangendorf, Real-world time-travel experiment shows ecosystem collapse due to anthropogenic climate change, Nat. Commun. 15 (2024) 1226.
[11] R. Semiat, Energy issues in desalination processes, Environ. Sci. Technol. 42 (2008) 8193–8201.
[12] S.M. Ali, A. Acquaye, An examination of water-energy-food nexus: from theory to application, Renew. Sustain. Energy Rev. 202 (2024) 114669.
[13] A. Pistocchi, T. Bleninger, C. Breyer, U. Caldera, C. Dorati, D. Ganora, M.M. Millán, C. Paton, D. Poullis, F.S. Herrero, M. Sapiano, R. Semiat, C. Sommariva, S. Yuece, G. Zaragoza, Can seawater desalination be a win-win fix to our water cycle? Water Res. 182 (2020) 115906.
[14] C. He, Z. Liu, J. Wu, X. Pan, Z. Fang, J. Li, B.A. Bryan, Future global urban water scarcity and potential solutions, Nat. Commun. 12 (2021) 4667.
[15] H. Quon, S. Jiang, Decision making for implementing non-traditional water sources: a review of challenges and potential solutions, npj Clean Water 6 (2023) 56.
[16] X. Xu, J.E. Ness, A. Miara, K.A. Sitterley, M. Talmadge, B. O'Neill, K. Coughlin, S. Akar, E.M.N.T. Edirisooriya, P. Kurup, N. Rao, J. Macknick, J.R. Stokes-Draut, P. Xu, Analysis of brackish water desalination for municipal uses: case studies on challenges and opportunities, ACS ES&T Eng. 2 (2022) 306–322.
[17] I. Shiklomanov, Chapter 2: world fresh water resources, in: P.H. Gleick (Ed.), Water in Crisis: A Guide to the World's Fresh Water Resources, Oxford University Pres, New York, 1993.
[18] S. Jasechko, D. Perrone, H. Seybold, Y. Fan, J.W. Kirchner, Groundwater level observations in 250,000 coastal US wells reveal scope of potential seawater intrusion, Nat. Commun. 11 (2020) 3229.
[19] B.R. Scanlon, S. Fakhreddine, A. Rateb, I. de Graaf, J. Famiglietti, T. Gleeson, R. Q. Grafton, E. Jobbagy, S. Kebede, S.R. Kolusu, L.F. Konikow, D. Long,

M. Mekonnen, H.M. Schmied, A. Mukherjee, A. MacDonald, R.C. Reedy, M. Shamsudduha, C.T. Simmons, A. Sun, R.G. Taylor, K.G. Villholth, C. J. Vörösmarty, C. Zheng, Global water resources and the role of groundwater in a resilient water future, Nat. Rev. Earth Environ. 4 (2023) 87–101.
[20] E. Jones, M. Qadir, M.T.H. van Vliet, V. Smakhtin, S.-M. Kang, The state of desalination and brine production: A global outlook, Sci. Total Environ. 657 (2019) 1343–1356.
[21] A. Al-Karaghouli, L.L. Kazmerski, Energy consumption and water production cost of conventional and renewable-energy-powered desalination processes, Renew. Sustain. Energy Rev. 24 (2013) 343–356.
[22] R. Singh, Chapter 6 - desalination and on-site energy for groundwater treatment in developing countries using fuel cells, in: N.P. Hankins, R. Singh (Eds.), Emerging Membrane Technology for Sustainable Water Treatment, Elsevier, Boston, 2016, pp. 135–162.
[23] H. Kariman, A. Shafieian, M. Khiadani, Small scale desalination technologies: a comprehensive review, Desalination 567 (2023) 116985.
[24] W. Liu, J.L. Livingston, L. Wang, Z. Wang, M. del Cerro, S.A. Younssi, R. Epsztein, M. Elimelech, S. Lin, Pressure-driven membrane desalination, Nature Reviews Methods Primers 4 (2024) 10.
[25] J.R. Du, X. Zhang, X. Feng, Y. Wu, F. Cheng, M.E.A. Ali, Desalination of high salinity brackish water by an NF-RO hybrid system, Desalination 491 (2020) 114445.
[26] P. Nativ, O. Leifman, O. Lahav, R. Epsztein, Desalinated brackish water with improved mineral composition using monovalent-selective nanofiltration followed by reverse osmosis, Desalination 520 (2021) 115364.
[27] P.M. Biesheuvel, S. Porada, M. Elimelech, J.E. Dykstra, Tutorial review of reverse osmosis and electrodialysis, J. Membr. Sci. 647 (2022) 120221.
[28] E.R. Nightingale, Phenomenological theory of ion solvation. Effective radii of hydrated ions, The Journal of Physical Chemistry 63 (1959) 1381–1387.
[29] S.H. Kim, S.-Y. Kwak, T. Suzuki, Positron annihilation spectroscopic evidence to demonstrate the flux-enhancement mechanism in morphology-controlled thin-film-composite (TFC) membrane, Environ. Sci. Technol. 39 (2005) 1764–1770.
[30] J. Xu, C. Zhu, Y. Wang, H. Li, Y. Huang, Y. Shen, J.S. Francisco, X.C. Zeng, S. Meng, Water transport through subnanopores in the ultimate size limit: mechanism from molecular dynamics, Nano Res. 12 (2019) 587–592.
[31] G.M. Geise, D.R. Paul, B.D. Freeman, Fundamental water and salt transport properties of polymeric materials, Prog. Polym. Sci. 39 (2014) 1–42.
[32] L. Wang, T. Cao, J.E. Dykstra, S. Porada, P.M. Biesheuvel, M. Elimelech, Salt and water transport in reverse osmosis membranes: beyond the solution-diffusion model, Environ. Sci. Technol. 55 (2021) 16665–16675.
[33] I. Shefer, O. Peer-Haim, R. Epsztein, Limited ion-ion selectivity of salt-rejecting membranes due to enthalpy-entropy compensation, Desalination 541 (2022) 116041.
[34] N. Kress, Chapter 2 - desalination technologies, in: N. Kress (Ed.), Marine Impacts of Seawater Desalination, Elsevier, 2019, pp. 11–34.
[35] K. Solonchenko, A. Kirichenko, K. Kirichenko, Stability of ion exchange membranes in electrodialysis, Membranes 13 (1) (2023) 52.
[36] M. Tedesco, H.V.M. Hamelers, P.M. Biesheuvel, Nernst-Planck transport theory for (reverse) electrodialysis: II. Effect of water transport through ion-exchange membranes, Journal of Membrane Science 531 (2017) 172–182.
[37] C. Jiang, Q. Wang, Y. Li, Y. Wang, T. Xu, Water electro-transport with hydrated cations in electrodialysis, Desalination 365 (2015) 204–212.
[38] S. Ozkul, J.J. van Daal, N.J.M. Kuipers, R.J.M. Bisselink, H. Bruning, J.E. Dykstra, H.H.M. Rijnaarts, Transport mechanisms in electrodialysis: the effect on selective ion transport in multi-ionic solutions, J. Membr. Sci. 665 (2023) 121114.
[39] M. Aliaskari, A.I. Schäfer, Nitrate, arsenic and fluoride removal by electrodialysis from brackish groundwater, Water Res. 190 (2021) 116683.
[40] M. Aliaskari, R.L. Ramos, A.I. Schäfer, Removal of arsenic and selenium from brackish water using electrodialysis for drinking water production, Desalination 548 (2023) 116298.
[41] S.-Y. Pan, A.Z. Haddad, A. Kumar, S.-W. Wang, Brackish water desalination using reverse osmosis and capacitive deionization at the water-energy nexus, Water Res. 183 (2020) 116064.
[42] P.K. Cornejo, M.V.E. Santana, D.R. Hokanson, J.R. Mihelcic, Q. Zhang, Carbon footprint of water reuse and desalination: a review of greenhouse gas emissions and estimation tools, Journal of Water Reuse and Desalination 4 (2014) 238–252.
[43] M. Vivar, S. H, M. Fuentes, Photovoltaic system adoption in water related technologies – a review, Renew. Sustain. Energy Rev. 189 (2024) 114004.
[44] Y.-A. Boussouga, B.S. Richards, A.I. Schäfer, Renewable energy powered membrane technology: system resilience under solar irradiance fluctuations during the treatment of fluoride-rich natural waters by different nanofiltration/reverse osmosis membranes, J. Membr. Sci. 617 (2021) 118452.
[45] W. He, A.-C. Le Henaff, S. Amrose, T. Buonassisi, I.M. Peters, A.G. Winter, Flexible batch electrodialysis for low-cost solar-powered brackish water desalination, Nature Water 2 (2024) 370–379.
[46] H. Xu, X. Ji, L. Wang, J. Huang, J. Han, Y. Wang, Performance study on a small-scale photovoltaic electrodialysis system for desalination, Renew. Energy 154 (2020) 1008–1013.
[47] M.W. Shahzad, M. Burhan, L. Ang, K.C. Ng, Energy-water-environment nexus underpinning future desalination sustainability, Desalination 413 (2017) 52–64.
[48] L. Wang, C. Violet, R.M. DuChanois, M. Elimelech, Derivation of the theoretical minimum energy of separation of desalination processes, J. Chem. Educ. 97 (2020) 4361–4369.
[49] F.E. Ahmed, R. Hashaikeh, N. Hilal, Hybrid technologies: the future of energy efficient desalination – A review, Desalination 495 (2020) 114659.
[50] H.B. Park, J. Kamcev, L.M. Robeson, M. Elimelech, B.D. Freeman, Maximizing the right stuff: the trade-off between membrane permeability and selectivity, Science 356 (2017) eaab0530.
[51] W. Song, M. Kumar, Beyond aquaporins: recent developments in artificial water channels, Langmuir 38 (2022) 9085–9091.
[52] K. Zuo, K. Wang, R.M. DuChanois, Q. Fang, E.M. Deemer, X. Huang, R. Xin, I. A. Said, Z. He, Y. Feng, W. Shane Walker, J. Lou, M. Elimelech, X. Huang, Q. Li, Selective membranes in water and wastewater treatment: role of advanced materials, Mater. Today 50 (2021) 516–532.
[53] J. Kim, K. Park, D.R. Yang, S. Hong, A comprehensive review of energy consumption of seawater reverse osmosis desalination plants, Appl. Energy 254 (2019) 113652.
[54] Q.J. Wei, R.K. McGovern, J.H. Lienhard V, Saving energy with an optimized two-stage reverse osmosis system vol. 3, Water Research & Technology, Environmental Science, 2017, pp. 659–670.
[55] M. Li, Optimal plant operation of brackish water reverse osmosis (BWRO) desalination, Desalination 293 (2012) 61–68.
[56] A.A. Atia, V. Fthenakis, Active-salinity-control reverse osmosis desalination as a flexible load resource, Desalination 468 (2019) 114062.
[57] B.G. Shah, V.K. Shahi, S.K. Thampy, R. Rangarajan, P.K. Ghosh, Comparative studies on performance of interpolymer and heterogeneous ion-exchange membranes for water desalination by electrodialysis, Desalination 172 (2005) 257–265.
[58] J. Zhao, Q. Chen, J. Wang, Novel ecofriendly cation exchange membranes for low-cost electrodialysis of brackish water: desalination and antiscaling performance, J. Membr. Sci. 661 (2022) 120908.
[59] K.M. Chehayeb, J.H. Lienhard, On the electrical operation of batch electrodialysis for reduced energy consumption, Environ. Sci.: Water Res. Technol. 5 (2019) 1172–1182.
[60] A. Campione, A. Cipollina, F. Calise, A. Tamburini, M. Galluzzo, G. Micale, Coupling electrodialysis desalination with photovoltaic and wind energy systems for energy storage: dynamic simulations and control strategy, Energ. Conver. Manage. 216 (2020) 112940.
[61] M.N. Soliman, F.Z. Guen, S.A. Ahmed, H. Saleem, M.J. Khalil, S.J. Zaidi, Energy consumption and environmental impact assessment of desalination plants and brine disposal strategies, Process Saf. Environ. Prot. 147 (2021) 589–608.
[62] N. Voutchkov, Desalination Engineering: Planning and Design, McGraw Hill Professional, 2012.
[63] S.K. Patel, M. Qin, W.S. Walker, M. Elimelech, Energy efficiency of electro-driven brackish water desalination: electrodialysis significantly outperforms membrane capacitive deionization, Environ. Sci. Technol. 54 (2020) 3663–3677.
[64] S.R. Shah, N.C. Wright, P.A. Nepsky, A.G. Winter, Cost-optimal design of a batch electrodialysis system for domestic desalination of brackish groundwater, Desalination 443 (2018) 198–211.
[65] E.L. Cussler, B.K. Dutta, On separation efficiency, AICHE J. 58 (2012) 3825–3831.
[66] M. Elimelech, W.A. Phillip, The Future of seawater desalination: Energy, technology, and the environment, Science 333 (2011) 712–717.
[67] A. Shrivastava, S. Rosenberg, M. Peery, Energy efficiency breakdown of reverse osmosis and its implications on future innovation roadmap for desalination, Desalination 368 (2015) 181–192.
[68] G. Doornbusch, M. van der Wal, M. Tedesco, J. Post, K. Nijmeijer, Z. Borneman, Multistage electrodialysis for desalination of natural seawater, Desalination 505 (2021) 114973.
[69] G.J. Doornbusch, M. Bel, M. Tedesco, J.W. Post, Z. Borneman, K. Nijmeijer, Effect of membrane area and membrane properties in multistage electrodialysis on seawater desalination performance, J. Membr. Sci. 611 (2020) 118303.
[70] S. Lin, Energy efficiency of desalination: fundamental insights from intuitive interpretation, Environ. Sci. Technol. 54 (2020) 76–84.
[71] S. Li, A. Voigt, A.I. Schäfer, B.S. Richards, Renewable energy powered membrane technology: energy buffering control system for improved resilience to periodic fluctuations of solar irradiance, Renew. Energy 149 (2020) 877–889.
[72] B.S. Richards, G.L. Park, T. Pietzsch, A.I. Schäfer, Renewable energy powered membrane technology: safe operating window of a brackish water desalination system, J. Membr. Sci. 468 (2014) 400–409.
[73] H. Strathmann, Chapter 4 - Operating Principle of Electrodialysis and Related Processes, Membrane Science and Technology, Elsevier, 2004.
[74] W. He, A.-C. Le Henaff, S. Amrose, T. Buonassisi, I.M. Peters, A.G. Winter, Voltage- and flow-controlled electrodialysis batch operation: flexible and optimized brackish water desalination, Desalination 500 (2021) 114837.
[75] E. Ogunniyi, B.S. Richards, Renewable energy powered membrane technology: power control management for enhanced photovoltaic-membrane system performance across multiple solar days, Appl. Energy 371 (2024) 123624.
[76] WHO, Guidelines for Drinking-water Quality: Fourth Edition Incorporating First Addendum (https://apps.who.int/iris/rest/bitstreams/1080656/retrieve access date 5/12/2022), 4th ed + 1st add ed., World Health Organization, Geneva, 2017.
[77] P. Długołęcki, B. Anet, S.J. Metz, K. Nijmeijer, M. Wessling, Transport limitations in ion exchange membranes at low salt concentrations, J. Membr. Sci. 346 (2010) 163–171.
[78] N. Mir, Y. Bicer, Integration of electrodialysis with renewable energy sources for sustainable freshwater production: a review, J. Environ. Manage. 289 (2021) 112496.
[79] DuPont, FILMTEC™ Reverse Osmosis Membranes, Technical Manual. https://www.dupont.com/content/dam/dupont/amer/us/en/water-solutions/public/documents/en/RO-NF-FilmTec-Manual-45-D01504-en.pdf, 2021. (Accessed 28 April 2021). Version 7.

[80] A. Matin, F. Rahman, H.Z. Shafi, S.M. Zubair, Scaling of reverse osmosis membranes used in water desalination: phenomena, impact, and control; future directions, Desalination 455 (2019) 135–157.
[81] B.S. Richards, J. Shen, A.I. Schäfer, Water–energy nexus perspectives in the context of photovoltaic-powered decentralized water treatment systems: a tanzanian case study, Energ. Technol. 5 (2017) 1112–1123.
[82] H. Ali, M.U. Siddiqui, M.A. Ammar, M. Aswani, M.I. Khan Umer, Techno-economic analysis of various configurations of stand-alone PV-RO systems for Pakistan, Renew. Energy 225 (2024) 120262.
[83] B.S. Richards, L. Masson, A.I. Schäfer, Impact of feedwater salinity on energy requirements of a small-scale membrane filtration system, in: E.K. Yanful (Ed.), Appropriate Technologies for Environmental Protection in the Developing World: Selected Papers From ERTEP 2007, July 17–19 2007, Ghana, Africa, Springer Netherlands, Dordrecht, 2009, pp. 123–137.
[84] A. Ruiz-García, I. Nuez, Long-term intermittent operation of a full-scale BWRO desalination plant, Desalination 489 (2020) 114526.